View metadata, citation and similar papers at core.ac.uk

brought to you by CORE

provided by NASA Technical Reports Server

3 1176 00150 2138

TECHNICAL MEMORANDUMS

NATIONAL ADVISORY COMMITTEE FOR AERONAUTICS

No. 791

BEHAVIOR OF TURBULENT BOUNDARY LAYERS ON CURVED CONVEX WALLS

By Hans Schmidbauer

Washington
April 1936

NATIONAL ADVISORY COMMITTEE FOR AERONAUTICS

TECHNICAL MEMORANDUM NO. 791

BEHAVIOR OF TURBULENT BOUNDARY LAYERS ON CURVED CONVEX WALLS*

By Hans Schmidbauer

SUMMARY

An approximate method for computing the friction layer at a plane plate for the case where the friction layer is simultaneously subject to a pressure gradient parallel to the plate, was presented by E. Gruschwitz in Ingenieur-Archiv II (1931). For a suitably chosen form parameter which indicated the approach of separation and the so-called "boundary-layer thickness," a system of linear differential equations was given by Gruschwitz.

This system of equations is here extended to take in the case where the friction layer is subject to centrifugal forces. Evaluation of the data yields a strong functional dependence of the momentum change and wall drag on the boundary-layer thickness radius of curvature ratio for the wall. It is further shown that the transition from laminar to turbulent flow occurs at somewhat higher Reynolds Numbers at the convex wall than at a flat plate, due to the stabilizing effect of the centrifugal forces.

The extended system of equations is applied to several boundary layers. For comparison, two examples for friction layers without curvature were also computed. It was found in each case that for a level plate the friction layer was about 25 percent thicker than that for a wall with convex curvature.

The work was undertaken at the Aerodynamic Institute of the Kaiser Wilhelm Gesellschaft at the suggestion of Dr. A. Betz. To him and to Dr. E. Gruschwitz I owe grateful acknowledgment for the much needed advice.

---

*"Verhalten turbulenter Reibungsschichten an erhaben gekrümmten Wanden." Thesis submitted in partial fulfillment of requirements for the degree of Doctor of Engineering in the Technischen Hochschule of Munchen, March 17, 1934.

I also desire to thank the Notgemeinschaft der deutschen Wissenschaft, with whose financial assistance the work was undertaken.

INTRODUCTION

The term "friction layer" is used to denote that portion of the flow near a streamline body, within which the frictional effect on the velocity of the fluid medium becomes of importance, this effect decreasing steadily to the value zero at the surface of the body. Any unevenness or discontinuities of the wall surface cause pressure disturbances within the boundary layer, which disappear quickly, however, for a small Reynolds Number. Flows having this property are the well-known laminar flows. On the other hand, when turbulent boundary layers, which set in at higher Reynolds Numbers, are considered numbers only, any such initial disturbances will rapidly increase in extent and consistently change the whole picture of the flow. To determine the Reynolds Number, we shall, in the present case, use as reference length the thickness of the disturbed layer; as reference velocity, will be taken the velocity of the undisturbed flow. Turbulent stream flows are by far much more frequent in engineering practice than the smooth laminar type, and for problems relating to lift and drag of airfoils are of the utmost importance.

On account of the irregularity of the motion that is superimposed on the main flow, the mathematical analysis of turbulent flow meets with considerable difficulty. We can, however, obtain good approximations for some cases, particularly for the more simple ones.

With the object of investigating the process which brings about the separation of friction layer and the consequent decrease in lift of an airfoil, E. Gruschwitz (reference 1) developed from his data an approximate method for computing the friction boundary layer for a plate in plane, rectilinear air flow. By placing walls of different forms opposite the plate, the effect of an increase or a decrease in pressure in the direction of flow on the friction layer of the plate could be observed.

Our object in this paper is to conduct a similar investigation on curved, convex walls of constant curvature so as to determine the effect of curvature on turbulent boundary layers.

As found by Wilcken (reference 2), the convex curvature has the effect of reducing the changes of momentum in the friction layer. At the same time, the layer on the convex side becomes thinner than that on the concave side, but due to the lessened turbulence becomes less capable of withstanding a pressure increase. This behavior of the layer may be explained by the fact that the faster particles, i.e., those farther removed from the wall, are subject to greater centrifugal forces than the slower ones. The faster particles tend to move farther off from the curved convex wall, thus effecting a separation. On hollow walls the effect is just the opposite; the stronger intermingling of the different fast particles increases the turbulence.

I. DESCRIPTION OF APPARATUS USED

A three-stage blower driven by a 10-horsepower motor forces the air through a pipe butt into a surge channel of from 60 to 65 cm cross-sectional area. The uneven velocity distribution is first smoothed out by a series of screens and straightened out by a "straightener." Passing through a nozzle-like constriction of the channel (the width, however, remaining 65 cm at all cross sections) the air finally reaches the place of measurement consisting of an upwardly curved channel between two parallel, perpendicular walls. The upper curved surface is the one from which measurements are taken, the curvature being constant. The experiments were made for three different radii of curvature: The series of measurements II to IV at $r = 25$ cm, series b to d at $r = 75$ cm, and series B to H at $r = 150$ cm. For the first case a complete cylinder was used as the inner side of the channel; for the two larger radii, cylinder sections of 150 cm arc length and 65 cm width, corresponding to the distance between the side walls were used.

The measuring walls were of strong sheet brass 1 mm thick. The channels with the 75 and 150 cm radius had a take-off run of 24 cm; along the middle of the channel there followed two rows of drilled holes, one row serving to introduce the pitot tubes and consisting of 17 holes of 2 mm diameter each and separated 80 mm from each other. The other row of drilled holes, at a lateral

---

cm × 0.3937 = in.; mm × 0.03937 = in.

distance of 30 mm from the first row, was used to measure the static pressure at the wall. There were 34 of these of 0.6 mm diameter each, spaced 40 mm apart. For the complete cylinder of 25 cm radius, only one pitot tube and pressure lead connection was necessary, since by turning the cylinder the measurement could be made at any point on the periphery.

The channel side opposite the measuring wall was made of strong sheet zinc 1 mm thick. Its form and the distance from the opposite side depended on the pressures desired in the channel. Since on account of the inconvenience, the pitot tube could be set in place only from underneath, the zinc surface was made revolvable about a front or rear axis as required. For some experiments, this surface was made up of interchangeable parts on account of the greater convenience. The slots in between were 3 mm wide. They were entirely suitable since they allowed the friction layer of the inner wall, which served no purpose in these experiments, free access to the outside.

Two upright plywood plates made up the sides of the channel. Windows in the wooden walls facilitated the insertion of the pitot tube and allowed the air flow to be observed by means of a silk streamer. A throttle was placed near the end of the channel. Due to the greater pressure in the channel, the friction layer of the oncoming air was forced out through an oblique slot, about 20 mm wide. In order to secure an initial boundary layer free from disturbance, a well rounded wood fillet was carefully fitted at the beginning of the measuring surface. The investigation was limited to the friction layer at the convex wall, since the outer wall was of variable curvature.

To measure the total pressure in the friction layer, steel pitot tubes of 0.6 mm outside diameter and 0.4 mm inside diameter were employed. They were soldered to a shaft of strong, 2 mm thick brass. Two kinds of pitot tubes of 20 and 60 mm length steel tubing were employed, so that with the 17 borings 80 mm apart, twice as many measuring stations 40 mm apart could be used. To allow for the curvature of the streamlines and to secure a better zero position on the wall, the steel tubes were bent slightly inward. At the flange above the holes a screw thread could be fastened to the pitot tube, allowing a change in depth of 0.01 mm to be easily read. The position at which the pitot tube touched the wall could be

well observed through the channel window on account of the reflecting brass wall. Since the pitot tube indicated the conditions prevailing in the center of the opening, its zero position actually corresponded to a point half the tube diameter away from the wall. The unused borings were suitably plugged. Total pressures were measured against the constant total pressure g_c of the undisturbed flow and read on a Prandtl (reference 3) manometer.

In order to smooth out small time variations of the pressure automatically, the steady flow channel was provided with a pressure regulating device of the type employed by O. Schrenk (reference 4). It consisted of a valve, loaded by a weight. This valve was held in suspension over an opening of the same size in the channel, by the undisturbed air forces. A small rise in pressure in the channel run raised the valve, causing an increased air flow, which in turn acted to oppose the pressure rise. The valve was so arranged that for large pressure variations, it struck against a projection above or below it as the case required, bringing a small auxiliary motor into action, which latter automatically changed the blower motor field, until a new equilibrium state was reached. By adjusting the regulating weight, any desired total pressure could be set up.

II. EXPERIMENTAL DATA

The totality of boundary-layer profiles obtained with a given channel form for a definite pressure range may be denoted as a "measurement series" (Messreihe). These series of measurements were named after the channel form used. In general, each curved channel form was investigated for only one velocity. Series III and IV were obtained with the same channel form, differing only in the velocities used. After the elimination of some initial experiments using "measuring series" I, a, A and C, in which the air flow became extremely irregular due to the fact that the channel was made too wide, the following 12 series of measurements remained:

"Measuring set" (channel form)	Radius (cm)	W_a (m/s)	R_{crit}	R_{max}
II	25	21.8	527	3640
Same form III	25	19.0	562	1690
Same form IV	25	31.0	505	4170
b	75	34.3	-	4820
c	75	34.3	-	5000
d	75	34.3	-	5800
B	150	25.5	548	3530
D	150	36.3	780	6700
E	150	36.2	530	4660
F	150	34.3	500	4490
G	150	33.2	530	-
H	150	40.0	787	6650

Channel form II can be deduced from figure 2. The common form for channels II and III is shown at the upper right-hand part of figure 1. The other channel forms are shown in figure 2.

Referring to the table, W_a denotes the air velocity at the end of the curved channel and $R = W \frac{\vartheta}{\upsilon}$ is the Reynolds Number (W is the velocity in the undisturbed air stream. ϑ is a measure of the boundary thickness defined farther on, υ is the kinematic viscosity of the air). R_{crit} is the value of the Reynolds Number at which the laminar layer becomes turbulent, and R_{max} is the Reynolds Number for the region of thickest boundary layer. Altogether, 16 series of measurements were used, comprising about 20 to 30 total-pressure profiles, each of which, on the average, was obtained for ten points. The evaluation of the data followed the prescribed method of Gruschwitz.

In the case of the "measurement series" IV, B (fig. 9), E, F (fig. 11), and G, the velocity profiles at the point of transition from laminar to turbulent flow, show that the separation of the smooth laminar layer from the wall has some effect on the occurrence of turbulence. For case II, the question could not definitely be decided. Sets b, c, and d were obtained under conditions where turbulence had already set in, the method of transition from laminar to turbulent flow not having been investigated for these cases.

In the single case of series G, a streamer at the middle of the measuring surface indicated a back flow in the region of farthest removal from the wall. The separation of the friction layer at the edges of the channel, where the opposing effects of two walls were superimposed, was confirmed for different measuring sets. To prevent the separation process from reaching over into the boundary layer at the measuring wall, two outlet slots were made between the outer wall and slots about 2 mm wide were made along the edges between the outer wall and side walls in some cases.

The velocity profiles obtained are similar to those of Gruschwitz, for comparison with which the profiles for sets II, b, d, B, F, and H are sufficient (figs. 3 to 17).

III. THE FRICTION LAYER

On account of the outlet slot used, a fresh boundary layer originated at the beginning of the measuring wall. It was therefore laminar at first, but sooner or later, depending on the pressure rise behind the constriction, it became turbulent.

1) System of coordinates, pressures, and velocities.- The friction layer was measured by determining the total pressure distribution at convenient distances along the periphery normal to the surface. The length of arc on the periphery in the flow direction was taken as the x coordinate and the distance normal to the surface as the y coordinate, both in centimeters. For channels b to d ($r = 75$ cm) and B to H ($r = 150$ cm), the point of impact at the rounded wood projection at the beginning of the curved inner wall was chosen as the origin of coordinates, the first measuring station being 18 cm away. For channels II to IV ($r = 25$ cm), the x origin was taken about 10 cm in front of the narrowest constriction, which was at the lowest part of the periphery.

As has already been mentioned, the constant total pressure head g_c outside the friction layer was chosen as reference pressure for the total head. g denotes the time average of the total pressure in the friction layer. It is made up, according to the well-known equation of energy for fluids, of the average dynamic pressure q in this layer and the average static pressure p. It is $g = q + p$.

With few exceptions, it was assumed that the static pressure within the friction layer was approximately constant and equal to the static pressure p_o at the wall. As shown by the above equation of energy for the layer, g is not constant, but on account of the friction losses, decreases in value as the wall is approached until the velocity contribution to the total head $\frac{\rho}{2} w^2 = q = g - p_o$ becomes zero; ρ is the air density, w the velocity in the layer.

Outside of this layer the air flow undergoes no losses. If we use the symbol δ to denote thickness of the friction layer, or the distance from the wall which may with sufficient accuracy be considered as separating the disturbed friction layer from the undisturbed region, then it is true that for $y \geq \delta$, the total head is $g = g_c =$ constant. For $y = \delta$, w becomes equal to W, the velocity corresponding to the dynamic pressure $q_\delta = \frac{\rho}{2} W^2 = g_c - p_o$. If the outside pressure p_a is put equal to zero in the equation applying to the cross section of the outlet, $\frac{\rho}{2} W_a^2 + p_a = g_c$, then g_c may be interpreted as the dynamic velocity at the end of the channel. In figures 3 to 17, the velocities were divided by W_a so as to obtain a nondimensional representation of the velocities in the friction layer.

Due to the well-known lack of suitable static-pressure indicators, the measurement of the static pressure within the friction layer is generally omitted. The pressure p_o at the wall is determined and assumed not to vary along the normal to the wall. This assumption holds strictly for plane walls with rectilinear stream flow, which is approximately the case as a rule. Although for curved walls this condition is not fulfilled, it is still allowable to neglect the variations in pressure provided the friction layer is sufficiently thin in comparison with the radius of curvature. For the series of measurements in which $r = 150$ cm was used, this condition was well fulfilled, whereas for the 75 cm radius, variation of the static pressure was already noticeable. The variation did not, however, influence the various magnitudes and deductions in any essential way.

The correction formula for the static pressure may be derived by the following simple consideration. The fluid

particles at any curved surface must follow a curved path, the resulting centrifugal forces being balanced by the pressure gradient $\partial p/\partial r$, where r is the streamline radius. Neglecting the small shearing forces, we may write:

$$\frac{\partial p}{\partial r} = \frac{\rho w^2}{r} = \frac{2(g-p)}{r}$$

The solution of this linear differential equation for p is

$$p = \left(\frac{r_o}{r}\right)^2 p_o + \frac{2}{r^2} \int_{r_o}^{r} g\, r\, dr$$

where p_o is the static pressure at the wall $(r = r_o)$. If we think of the streamlines within a small region as represented by concentric circles, we may put $r = r_o + y$. Since y is small compared with r_o, we may put $(r_o/r)^2$ approximately equal to $1/\left(\frac{1+2y}{r_o}\right)$ and in the second member of the equation set $r = r_o$. Let $k_o = \frac{1}{r_o}$ denote the curvature at the wall. The corrected formula for the static pressure will then assume the form

$$p \approx \frac{p_o}{1 + 2k_o y} + 2k_o \int_{o}^{y} g\, dy$$

2) Effect of secondary flow on the friction layer.- A characteristic of curved channels is the setting up of secondary flow. This is connected with the fact that, due to the curvature there is a pressure drop directed inward. In a channel with rectangular cross section, this radial pressure gradient acts directly only on the friction layer at the plane side walls, forcing the liquid particles toward the inside, according to the amount of their loss in kinetic energy. As a result of the increase in the slowed-up material, the friction layer becomes thicker there, while at the outer wall it becomes thinner. Under certain conditions this transport of particles in the friction layer may affect the entire flow, in which case two oppositely directed vortices will be built up which will be superimposed on the main flow and constitute a secondary flow. It is to be noted that this process affects the thickness of the friction layer in just the opposite way

to the purely centrifugal effects investigated by Wilcken and mentioned in the Introduction. The present investigation deals only with the latter and therefore by secondary flow will be eliminated as far as possible by using channel forms of suitable cross sections. It was not always possible, owing to the necessity of maintaining a proper distance for the pressure gradient to build up, to utilize the best form of cross-sectional area which in the ideal case would be a long narrow rectangle with its smaller side directed radially, so that in a few cases with specially unfavorable cross-sectional form or strong curvature as, for example, channels II, III, and IV, secondary flow effects may be assumed to have occurred.

3) The results obtained for the friction layer of a flat plate.- The object of this treatise is to show quantitatively how centrifugal forces affect a boundary layer which is at the same time subject to a pressure gradient in the direction of flow. As has already been mentioned, Gruschwitz's calculations were used as a basis for this work. More particularly, an attempt was made to determine how the two approximate differential equations for his experiments were to be modified so as to take the curvature effect into account. It will be useful therefore to describe briefly the procedure employed by Gruschwitz.

In measurements taken on boundary layers, the "displaced air thickness" δ^+ is often used as a measure of the layer thickness. This quantity is defined by the equation

$$\delta^+ = \int_0^\infty \left(1 - \frac{w}{W}\right) dy$$

An additional measure of the layer thickness is introduced by Gruschwitz, the length ϑ, defined by the equation

$$\vartheta = \int_0^\infty \frac{w\,(W - w)}{W^2}\, dy$$

It is a measure of the loss of momentum in the friction layer.

To give a complete description of a boundary profile, Gruschwitz introduces besides ϑ, a form parameter η, and defines it, for any distance from the wall $y_1 = \vartheta$, as

$$\eta = 1 - \left(\frac{w_1}{W}\right)^2$$

This expression may be written $\eta = (q_\delta - q_1)/q_\delta$ and assumes the form

$$\eta = \frac{g_\delta - g_1}{q_\delta} \tag{1}$$

when the variation of the static pressure along the normal to the surface is negligible. The subscripts 1 are used to indicate the values of the magnitudes w, q, and g at the distance ϑ, from the wall.

Still another magnitude $H = \delta^+/\vartheta$ is employed, which, like η, may be interpreted as a form parameter. From his data, Gruschwitz found the functional relation $H = f(\eta)$. The dependence is shown in figure 18.

With the aid of some dimensional considerations, Gruschwitz found on the basis of his measurements the following relation for the turbulent friction layer

$$\frac{\vartheta}{q_\delta}\frac{dg_1}{dx} = \eta\ 0.00894 - 0.00461 \tag{2}$$

graphically shown in figure 19 (his value q being identical with q_δ).

Putting the value of η from (1) in equation (2), we get

$$\vartheta\frac{d(q_\delta\ \eta)}{dx} = -\ q_\delta\ \eta\ 0.00894 + q_\delta\ 0.00461 \tag{3}$$

Application of von Karman's (reference 5) principle of momentum to the friction layer, yields a second relation:

$$\frac{d\vartheta}{dx} + \frac{H+2}{2}\frac{\vartheta}{q_\delta}\frac{dq_\delta}{dx} = \frac{\tau_o}{\rho W^2} \tag{4}$$

wherein τ_o is the shearing stress at the wall. For the simplest type of flow the well-known relation for the shearing stress $\tau = \mu\frac{dw}{dy}$ holds true. As may be seen from this expression, the viscosity and the velocity profile both enter into this expression. It is possible, therefore, to express the nondimensional shearing stress $\tau_o/\rho W^2$ too, as a function of the Reynolds Number and the form parameter η. Gruschwitz, using certain approxima-

tions, found a good agreement for the measured and computed value of ϑ by setting $\frac{\tau_0}{\rho W^2} = 0.002$. If it is further assumed that H is constant, then equations (3) and (4) will constitute a pair of differential equations, in which η and ϑ are the only unknown variables.

4) Some dimensional considerations and results of measurements on the friction layer at curved walls.- To obtain a quantitative measure of the effect of the curvature, it is not sufficient to follow merely the changes in the layer thickness. Since there is some likelihood for secondary flow to occur, it is extremely important to get a picture of the entire profile changes occurring within the friction layer; that is to say, follow the changes in η. Since η has been defined for the distance ϑ measured from the wall, it will be useful, following Gruschwitz, to consider the dimensional relations for a fluid particle at a distance ϑ.

The line $y = \vartheta$ follows approximately a streamline direction, so that the equation of motion for a particle at distance ϑ ought first to be considered.

It may be assumed that the changes of momentum undergone by the particle in its turbulent motion will be a function of its proper velocity w_1, its distance from the wall ϑ, the velocity of the undisturbed flow W, and the physical constants of the fluid, namely, the viscosity μ, and the density ρ. For a curved surface, there is the additional factor r, the radius of curvature of the wall. Near the wall, the streamline length ds may be replaced by dx, so that the approximate equation of motion along the line $y = \vartheta$ will be:

$$\frac{dp}{dx} + \rho\, w_1 \frac{dw_1}{dx} = f(w_1, W, \vartheta, r, \mu, \rho)$$

Since for the total pressure the relation $g = p + \rho\, w^2/2$ holds in general, the above equation may be written in the simplified form as

$$\frac{dg_1}{dx} = f(w_1, W, \vartheta, r, \mu, \rho).$$

According to mathematical theory, it is always possible, out of n given magnitudes occurring in any equation, to

derive (n - 3) independent nondimensional magnitudes. Here we may use the four expressions $\frac{\vartheta}{q_\delta}\frac{dg_1}{dx}$, $\eta = 1 - (w_1/W)^2$, ϑ/r, and $R = W\frac{\vartheta}{\nu}$ ($\nu = \mu/\rho$ is the kinematic viscosity), so that the above relation may be written:

$$\frac{\vartheta}{q_\delta}\frac{dg_1}{dx} = f(\eta, \frac{\vartheta}{r}, R)$$

The dependence of $\frac{dg_1}{dx}$ on R could not be determined with sufficient accuracy. It may, however, be assumed that the true viscosity μ is generally negligibly small compared to the apparent viscosity which results from the turbulent motion. With this proviso, the above relation is further simplified to the expression:

$$\frac{\vartheta}{q_\delta}\frac{dg_1}{dx} = f\left(\eta, \frac{\vartheta}{r}\right) \qquad (5)$$

The derivative was plotted against η, as shown by the examples in figures 20 and 21, for each channel form, and the curves show a certain regularity.

Figure 22 shows all the test results obtained. The singular case for the plane plate, $r = \infty$, is represented by the straight line $\vartheta/r = 0$. The choice of different symbols makes it easier to distinguish the several channel forms on the diagram. The increase or decrease of the friction layer may be deduced from an inspection of the figure from the values of ϑ/r indicated on the series of straight lines.

The curves begin at the right of the line $\frac{\vartheta}{r} = 0$ with values of η ranging from 0.5 to 0.7, and rise upward and to the right, as explained by the dynamic pressure q_δ, and therefore, as also shown by figures 24 to 35, the length ϑ increases with increase of the form parameter η, for the first section of the measured distance (that is, the distance from the wall).

The distribution of the test values (fig. 22) shows in a striking manner that the preponderant majority of the $\frac{\vartheta}{q_\delta}\frac{dg_1}{dx}$ values are lower than those obtained by Gruschwitz

$\left(\frac{\vartheta}{r} = 0\right)$. The explanation is provided by a consideration of the equation of motion:

$$\frac{dg_1}{dx} = \frac{dp}{dx} + \rho\, w_1 \frac{dw_1}{dx}$$

Since, evidently, $\rho\, w_1 \frac{dw_1}{dx}$ may be expressed as the time rate of change of the momentum, $\frac{d(\rho\, w_1)}{dt}$, dg_1/dx may be taken as a measure of the changes in momentum of the fluid particle at the distance y_1 $(= \vartheta)$ from the wall. As has been mentioned in the Introduction, the changes in momentum at the inner wall of the channel must be less than those at the hollow side. We may assume then that the region above the straight line $\vartheta/r = 0$ represents the friction layer at curved concave walls.

The smaller w_1 is compared to W, the larger the value of η. When a definite limit is exceeded, the kinetic energy in the friction layer will no longer be able to withstand the pressure increase and separation sets in. According to the results of Gruschwitz (fig. 19), there is a sudden decrease in the values of η in the neighborhood of $\eta = 0.8$. From this, Gruschwitz concluded that the separation occurs for this value. If we examine his velocity profiles, we are struck by the fact that the profile forms in the region of $\eta = 0.8$; for example, those of his measuring set 5, are far from indicating any oncoming separation. The form of these profiles indicates a far greater probability of the occurrence of separation at values of η greater than 0.8, as long as it is taken care that the pressure gradient in this region is not too steep.

This conjecture is confirmed by the profile forms shown in figure 22; for example, those of channel H. The occurrence of separation should accordingly be expected for values of $\eta = 0.9$ and above in the region of a low-pressure gradient, and high values of η be expected for values of $\eta = 0.9$ and above. With channel H, for example, a value of $\eta = 0.95$ (fig. 35) was attained without any apparent separation; yet, as was indicated by the fluttering streamer, the condition was well nigh reached. The small hump, for example, of the velocity profile $x =$ 90 cm (fig. 16) showed that the turbulent fluctuations had already become so large that the measurements near the wall were considerably in error.

In general, it may be said that for turbulent boundary layers the pitot tube measures the time average of the fluctuations. If these fluctuations exceed the main motion, however, upon which they are superimposed, as may happen just before separation occurs, the pitot tube will at times be exposed to back flow. Since in this case the pitot tube indicates too low a pressure, the average time value is measured too high, accounting for the hump in the profile. The true pressure decrease for the profile x = 90 cm (fig. 16) should approximately correspond to the dotted line, which clearly indicates the conditions before separation. Since it is often difficult to obtain the derivative dg_1/dx, the ordinates in figures 20 to 22 are affected with some degree of uncertainty.

5) The differential equations for the friction layer modified to take the curvature into account.- A certain regularity in the distribution of the ϑ/r values may clearly be seen. The parameter ϑ/r increases with increasing distance from the straight line $\frac{\vartheta}{r} = 0$ of Gruschwitz. An attempt was made to interpolate all points with equal values for ϑ/r by straight lines. The straight lines were found to pass through a common intersection point whose coordinates were $\eta = -0.1$, $\frac{\vartheta}{q_\delta}\frac{dg_1}{dx} = -0.0055$.

As shown in figures 20 to 22 and as might have been expected from the narrowing of the latter part of the channel form, the values ϑ/r again decrease when the curves drop from their maximum values toward the left. While the ϑ/r values do not fall on a system of straight lines, yet for steady decrease pressure this tendency was clearly seen. No satisfactory explanation for the deviation could be found.

If the angle that the straight lines form with the x axis be denoted by φ, the equation for the system of straight lines may be written:

$$\frac{\vartheta}{q_\delta}\frac{dg_1}{dx} = \tan\varphi\,(\eta + 0.1) - 0.0055 \qquad (6)$$

A good approximate formula for the ϑ/r system, was found to be:

$$\tan\varphi = 0.00894 - 0.315\,\frac{\vartheta}{r} \qquad (7)$$

Substituting this value of $\tan \varphi$ from (7) into equation (6), we obtain:

$$\frac{\vartheta}{q_\delta} \frac{dg_1}{dx} = (\eta + 0.1)\left(0.00894 - 0.315 \frac{\vartheta}{r}\right) - 0.0055 \quad (8)$$

From (1) $g_1 = - q_\delta \eta + g_c$. Differentiating this expression with respect to x and substituting in (8) the final equation is obtained:

$$\frac{d(q_\delta \eta)}{dx} = \frac{1}{\vartheta}\left(-(q_\delta \eta + 0.1\ q_\delta)(0.00894 - 0.315 \frac{\vartheta}{r}) + 0.0055\ q_\delta\right) \quad (9)$$

For the unknown variable ϑ in this equation, it is again assumed that relation (4) holds:

$$\frac{d\vartheta}{dx} + \frac{H + 2}{2} \frac{\vartheta}{q_\delta} \frac{dq_\delta}{dx} = \frac{\tau_o}{\rho W^2}$$

It has already been pointed out that the right member of this equation depends to a slight degree only on R and η. It should likewise be noted that in this form of the equation, the effect of curvature is not accounted for. To avoid a tedious transformation into cylindrical coordinates, this effect was determined from the experimental data. For this purpose such ranges of experimental values were used as to allow the calculation of the derivatives $d\vartheta/dx$ and dq_δ/dx with some degree of accuracy. In this manner, the left-hand side of equation (4) was computed point by point and the values of $\tau_o/\rho W^2$ with the corresponding ϑ/r values obtained, as shown in figure 23.

Since $\tau_o/\rho W^2$ is, however, computed as the difference of the two derivatives, its evaluation is in considerable doubt, so that on the experimental basis alone it cannot be definitely asserted that the shearing stress does not depend on R and η. Moreover, in the region of the built-up turbulence, only values of η between 0.5 and 0.85 are at our disposal. For larger pressure rises, this uncertainty is of small practical importance, as the shearing-stress component is relatively small compared to the pressure component. The dropping of the curve with increasing ϑ/r corresponds to the rapidly increasing momentum changes.

6) The computation process applied to the friction layer.- As described recently by Gruschwitz, the linear differential equations (4) and (9) may conveniently be integrated graphically following a method by Czuber (reference 6), in which the true integral curves ϑ and η are approximated by straight chords.

The transition from laminar to turbulent flow does not occur regularly at the same place but at continually varying positions within a narrow region. To determine the initial values of ϑ and η where the turbulent layer begins, it is assumed that the transition originates at a definite position, and for an undisturbed "momentum flow" under this idealized condition to be maintained, it is necessary that the initial value of ϑ for turbulent flow be equal to the final value for laminar flow. The laminar boundary layer may be approximately determined by the method of Kármán-Pohlhausen (reference 7). For the η range of values, Gruschwitz found good agreement with the measured values when $\eta = 0.1$ is chosen as the initial value. For our case the same initial value was found to be good.

As a first approximation for ϑ, it may be assumed that the relation for the thickness $H = \delta^+/\vartheta$ is constant for all profiles, so that $H = f(\eta)$ is constant in equation (4), an average value of $H = 1.5$ being found suitable. The ϑ values thus found and the known pressure distribution enable equation (9) to be solved by the same graphical method that was used for equation (4). Having found the values for η, the more accurate values of $H = f(\eta)$ are read off from figure 18 and again substituted in equation (4) for a second approximation for ϑ. The new values for ϑ are used to obtain a second approximation for η from equation (9), and so on. Two approximations are all that is necessary; in fact, the first approximation is generally close enough.

Difficulty is encountered when the above process is applied to find the point of transition from laminar to turbulent flow, since the Reynolds Number does not stay constant at this critical point but fluctuates between definite limits. As the table previously given shows, the critical Reynolds Number values lie somewhere between 500 and 790. Where separation occurred, a value between 500 and 550 was found. Due to the steadying influence of the centrifugal forces, a somewhat higher value was found than for the case of the level plate. No relation between the Reynolds

Number and ϑ/r or $\frac{\vartheta}{q_\delta}\frac{dp}{dx}$ could be definitely established.

Figures 24 to 35 show ϑ, η and p_o/g_c as functions of x, the distance along the measured surface. For series b, B, E, and F the approximate computations were carried through. The transition point for the series of measurements b was not measured. For comparison, the p_o/g_c values for a level plate were computed and are shown on the figures for series E and F. As may be seen, there is an increase in the ϑ_{max} value of about 25 percent. For series II, III, and IV, there was agreement between the measured and computed values of ϑ/r up to about 0.003; thereafter, the measured ϑ values were considerably greater than the computed values. The reason for this difference may appear from the fact that the strong curvature and unfavorable cross-sectional area of the channels used for these measurements made it difficult to avoid secondary flow.

Translation by S. Reiss,
National Advisory Committee
for Aeronautics.

REFERENCES

1. Gruschwitz, E.: The Process of Separation in the Turbulent Friction Layer. T.M. No. 699, N.A.C.A., 1933.

2. Wilcken, H.: Turbulente Grenzschichten an gewölbten Flächen. Ing.-Archiv I (1930), p. 357.

3. Ergebnisse der aerodynamischen Versuchsanstalt zu Göttingen, I. Lieferung, München, 1921.

4. Schrenk, O.: Ing.-Archiv I (1930), p. 350.

5. von Karman, Th.: Über laminare und turbulente Reibung. Z.f.a.M.M. I (1921), p. 233.

6. Czuber, E.: Z. f. Math. u. Phys. 44 (1899), p. 41; also

   Hort, W.: Die Differentialgleichungen des Ingenieurs, Berlin, 1925, p. 237.

7. Pohlhausen, K.: Zur näherungsweisen Integration der Differentialgleichung der laminaren Grenzschicht. Z.f.a.M.M. I (1921), p. 252.

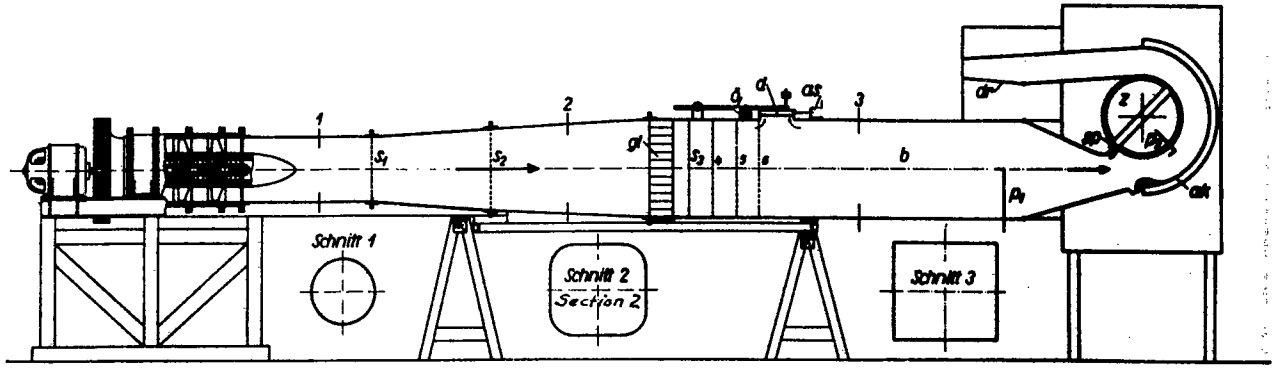

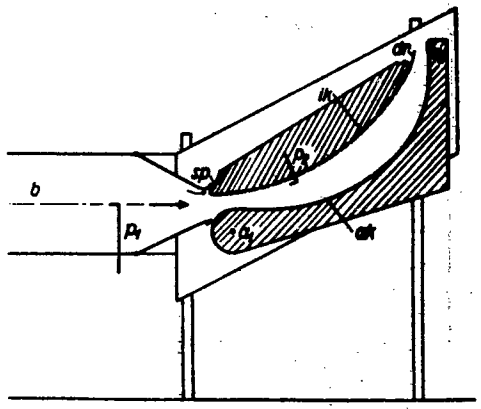

Figure 1.- s_1 to s_6 screens, gl honeycomb, b channel of steady flow, d cover of pressure regulator, o oil damper, as regulator cover stop, p pitot tube to measure total pressure head g_c in undisturbed flow, p_2 replaceable pitot tube to measure the variable total pressure head in the boundary layer, sp blow-off vent, z cylinder, ak outer wall of channel, ik and z inner wall, a_1 and a_2 axes of curved wall ak, dr throttle.

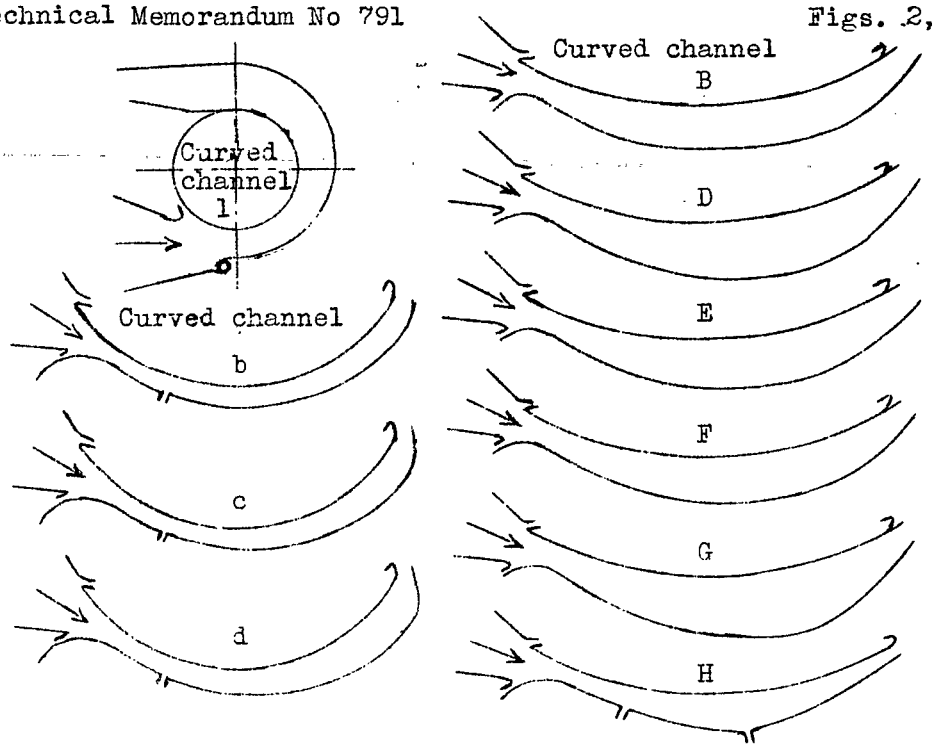

Figure 2.- Channel forms (see fig. 1 for set up).

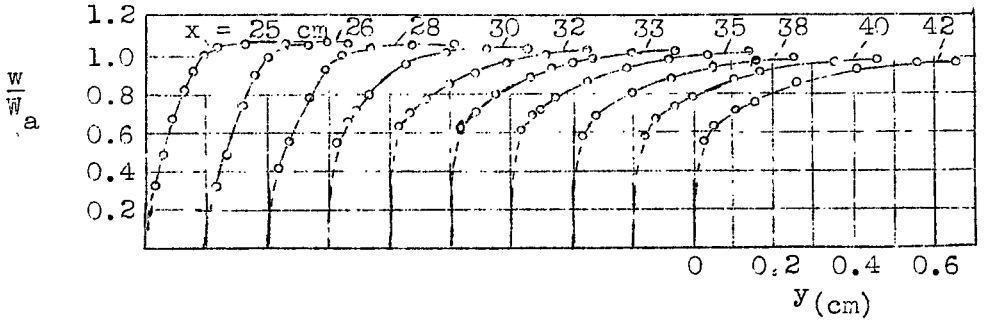

Figure 3.- Velocity profiles for set of measurements II.

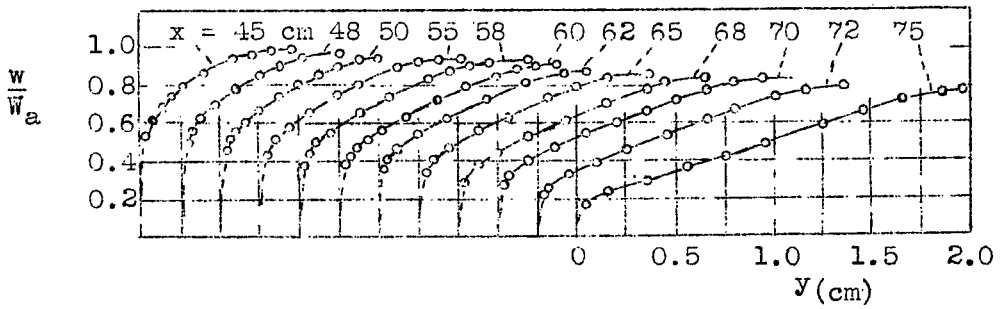

Figure 4.- Velocity profiles for set of measurements II.

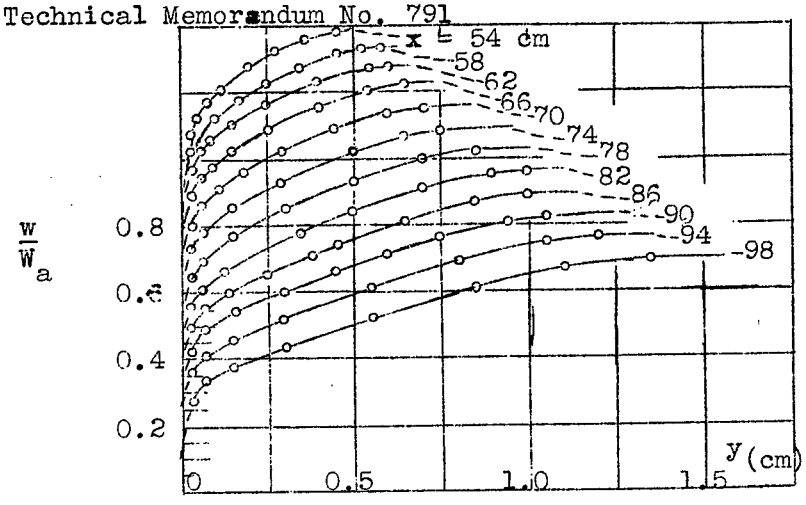

Figure 5.- Velocity profiles for set of measurements b

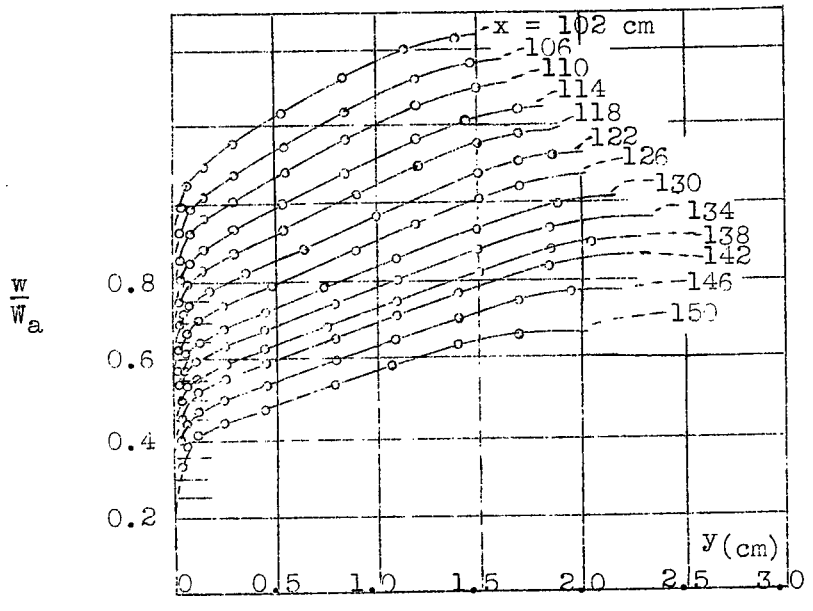

Figure 6.- Velocity profiles for set of measurements b

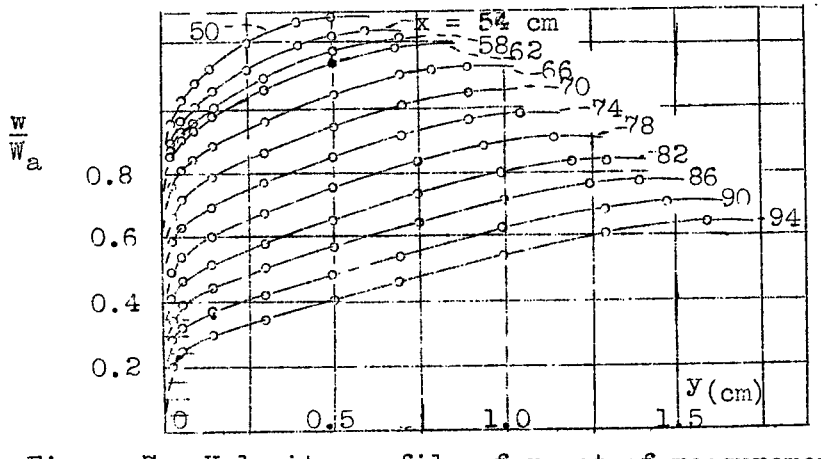

Figure 7.- Velocity profiles for set of measurements d

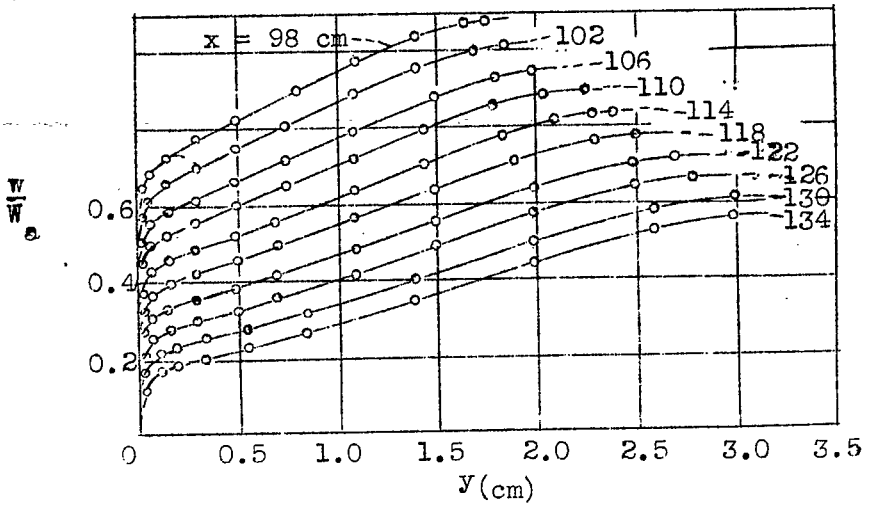

Figure 8.- Velocity profiles for set of measurements d

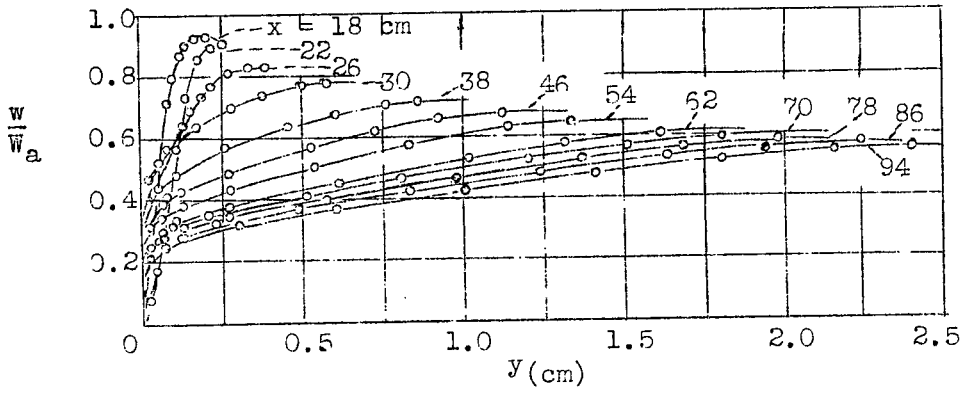

Figure 9.- Velocity profiles for set of measurements B

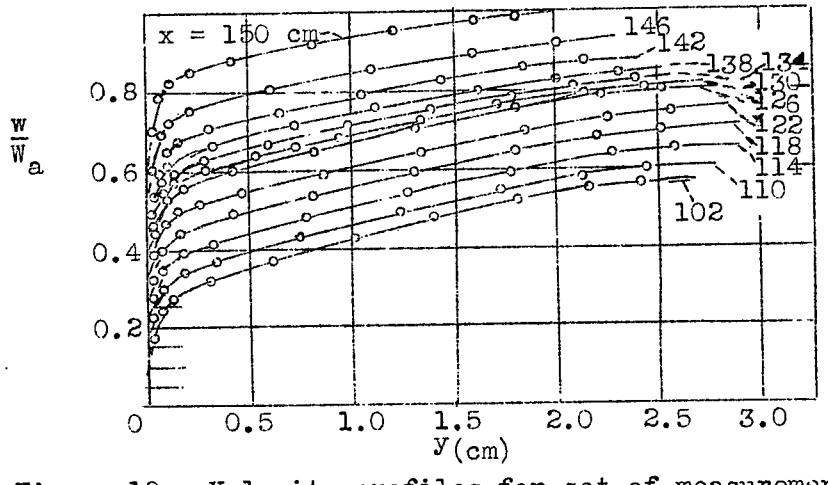

Figure 10.- Velocity profiles for set of measurements B

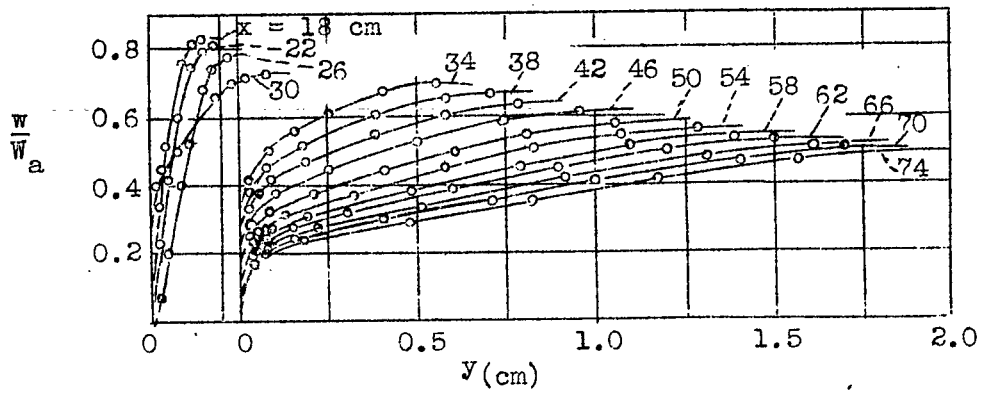

Figure 11.- Velocity profiles for set of measurements F

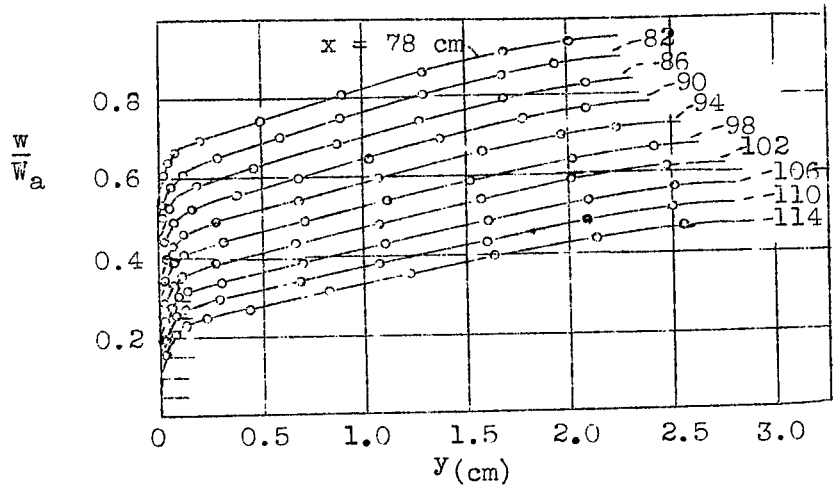

Figure 12.- Velocity profiles for set of measurements F

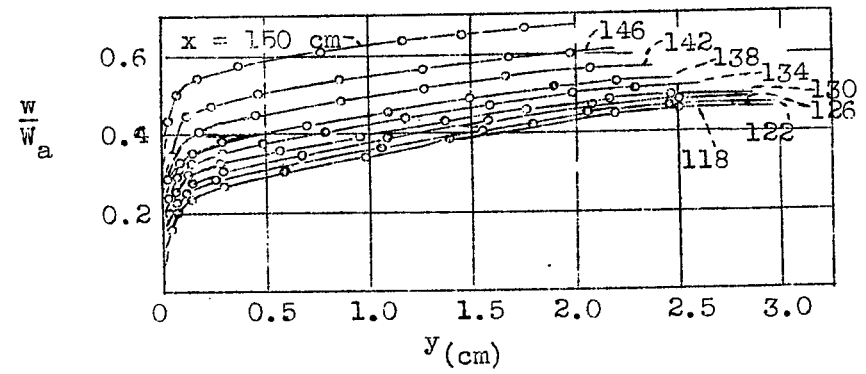

Figure 13.- Velocity profiles for set of measurements F

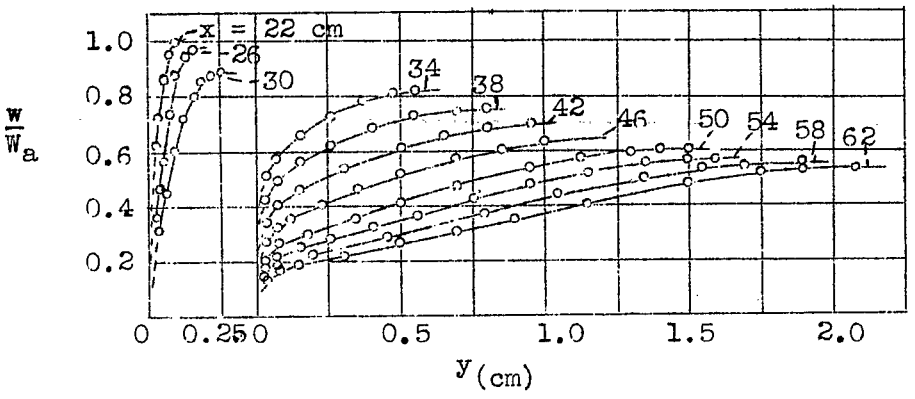

Figure 14.- Velocity profiles for set of measurements H

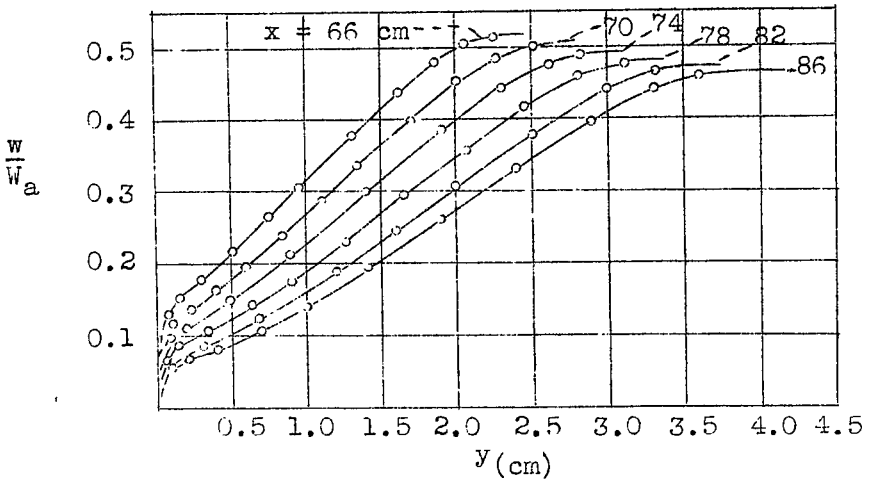

Figure 15.- Velocity profiles for set of measurements H

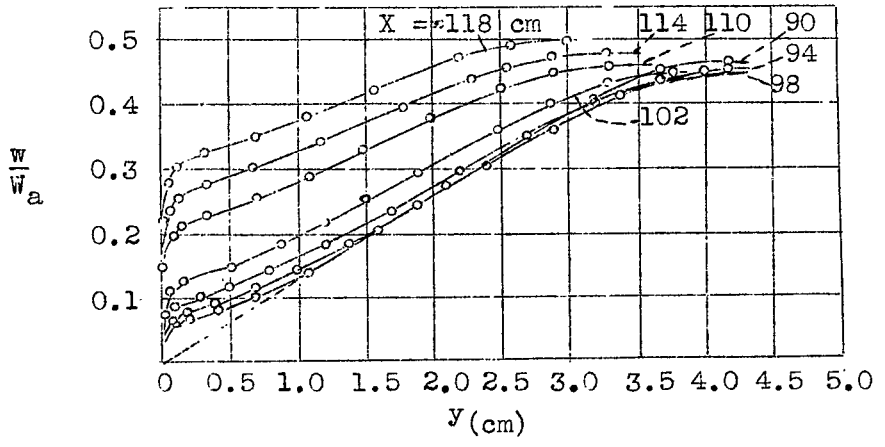

Figure 16.- Velocity profiles for set of measurements H

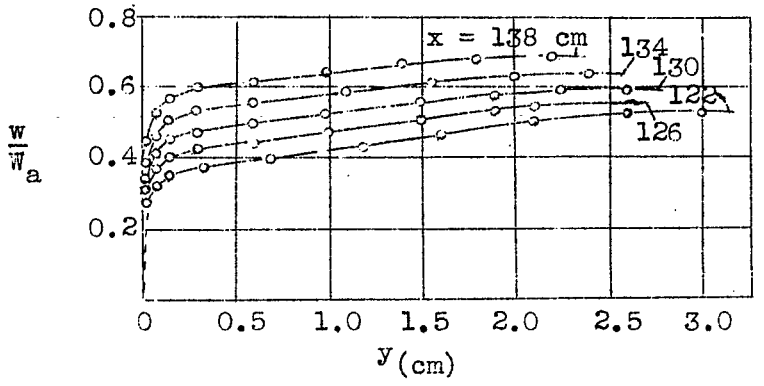

Figure 17.- Velocity profiles for set of measurements H

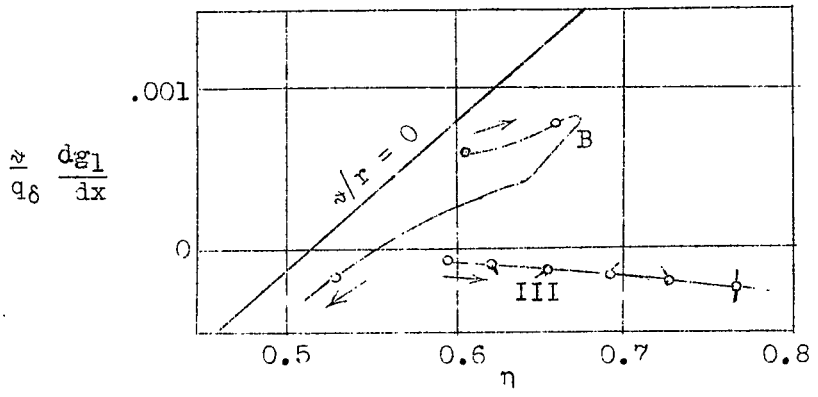

cm × .3937 = in.

Figure 20.- Measurements in the turbulent boundary layer at the inner wall of channel forms III (r = 25 cm) and B (r = 150 cm). For notation see fig. 22.

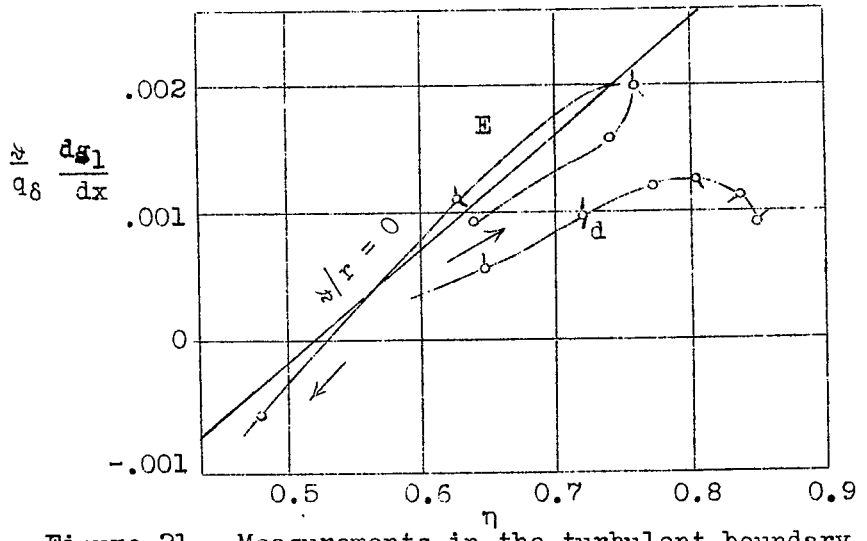

Figure 21.- Measurements in the turbulent boundary layer at the inner wall of channel forms d (r = 75 cm) and E (r = 150 cm). For notation see fig. 22.

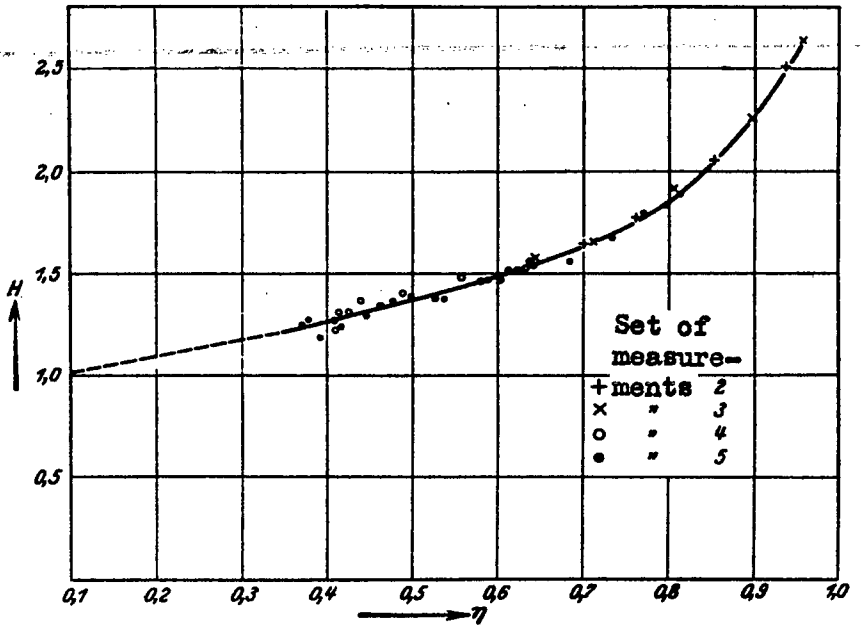

Figure 18.- Ordinates $H = \delta^*/\vartheta$, abscissa $\eta = 1-(w_1/W)^2$

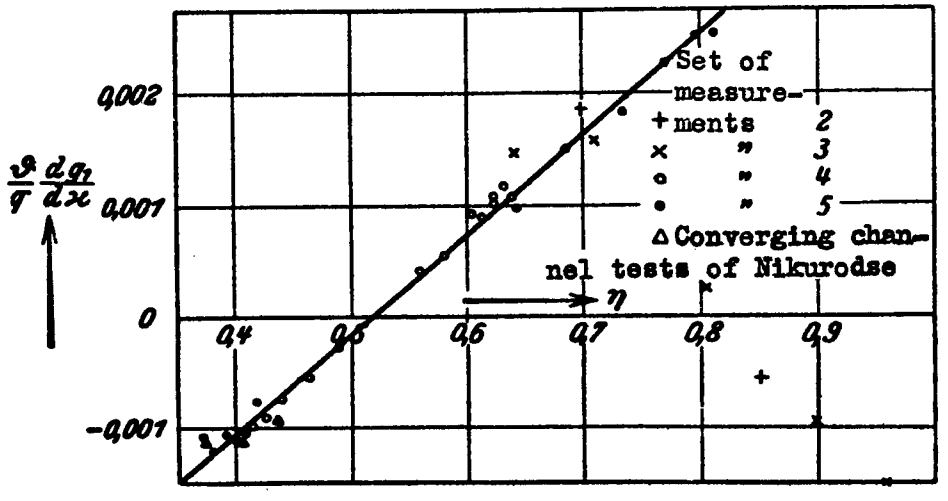

Figure 19.- Test results of Gruschwitz on flat plates.

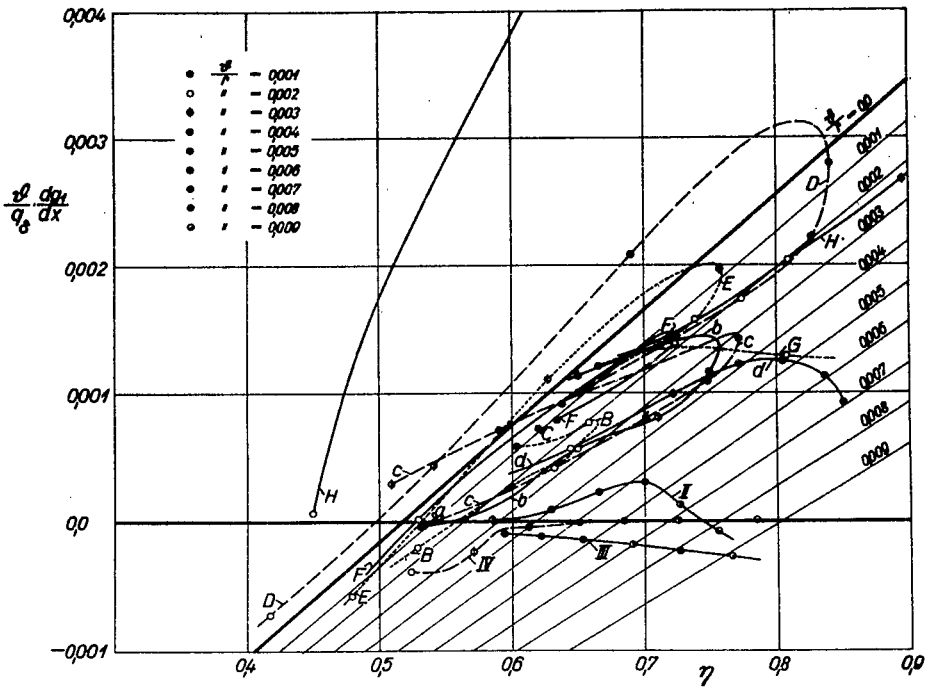

Figure 22.- Tests results on convex curved walls.

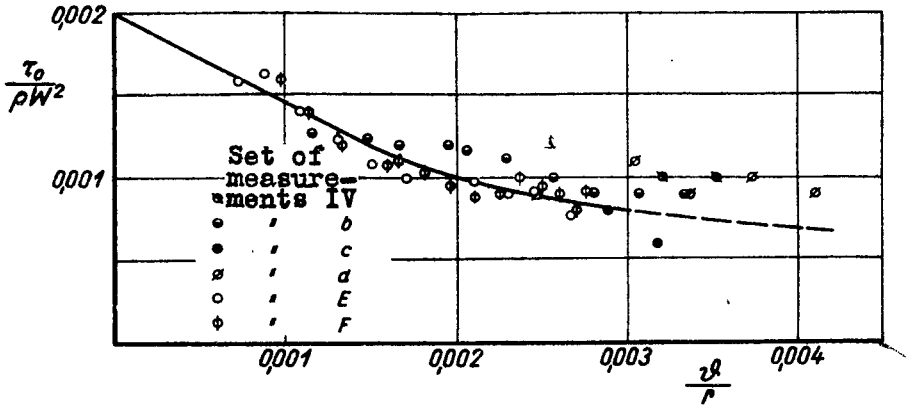

Figure 23.- Ordinates $\tau_o/\rho W^2$, abscissa ϑ/r

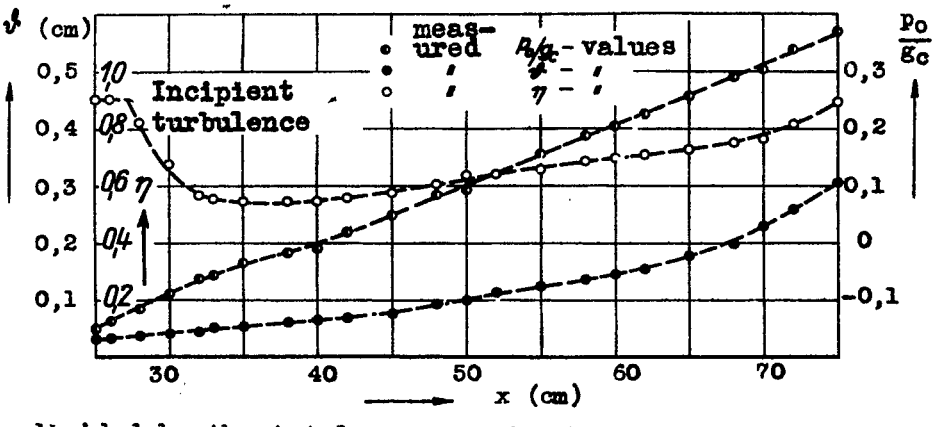

Figure 24.- Set of measurements II. Thickness of friction layer ϑ, form parameter η, and static pressure at wall p_o plotted against distance along inner wall circumference x. (p_o is divided by the total pressure head q_c at the undisturbed flow to obtain a non-dimensional value).

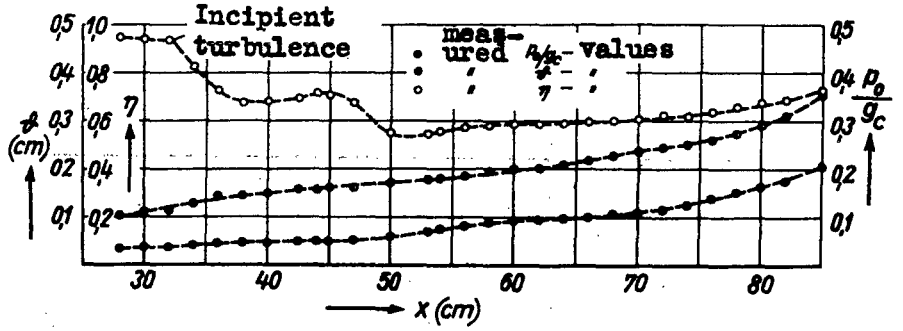

Figure 25.- Set of measurements III.

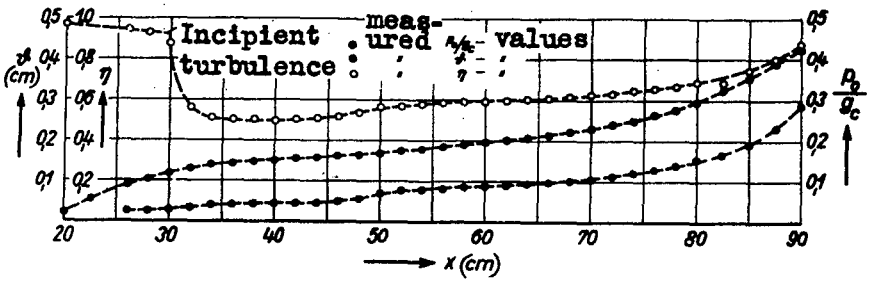

Figure 26.- Set of measurements IV.

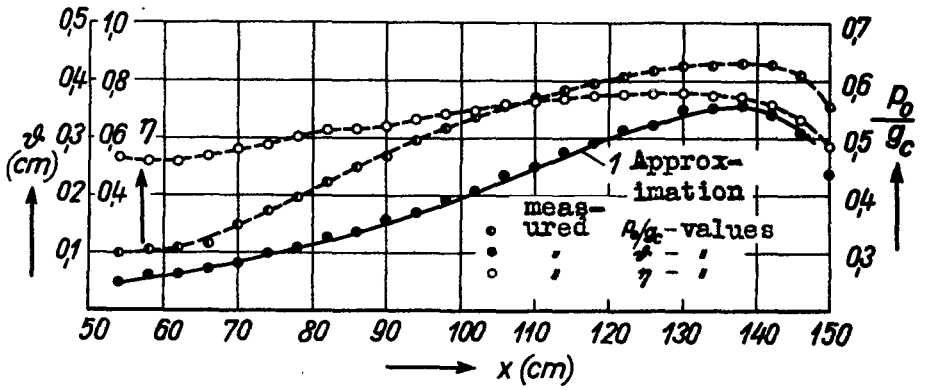

Figure 27.- Set of measurements b.

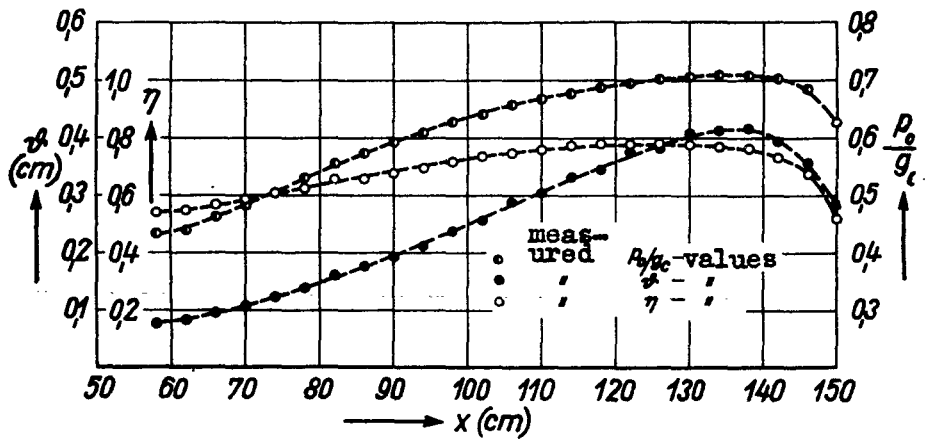

Figure 28.- Set of measurements c.

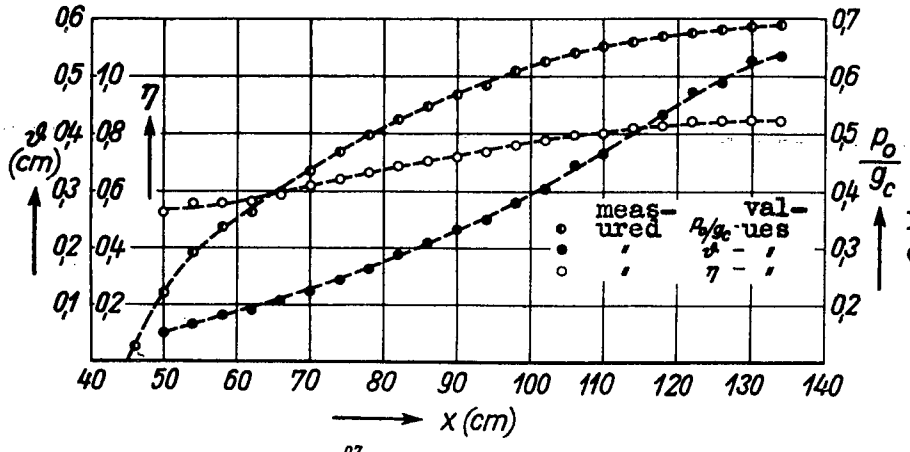

Figure 29.- Set of measurements d

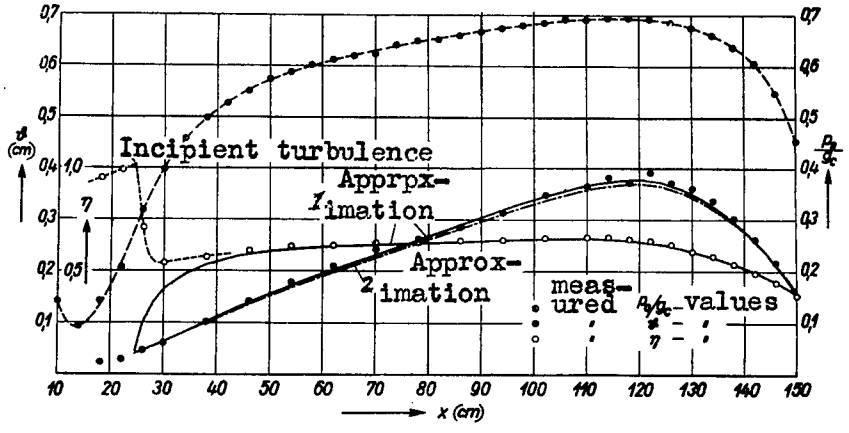

Figure 30.- Set of measurements B

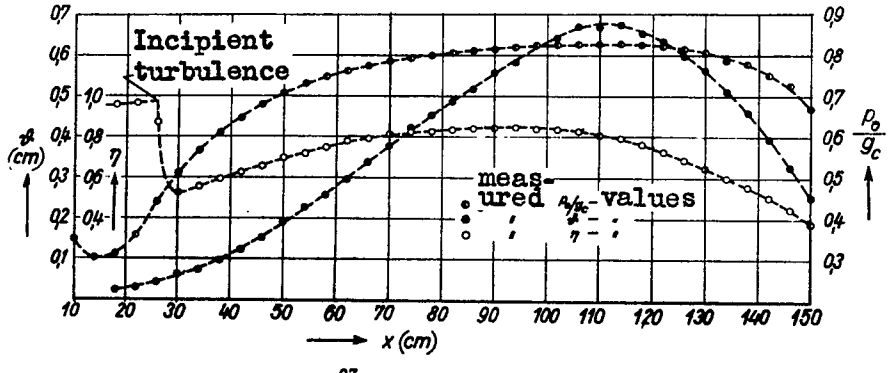

Figure 31.- Set of measurements D

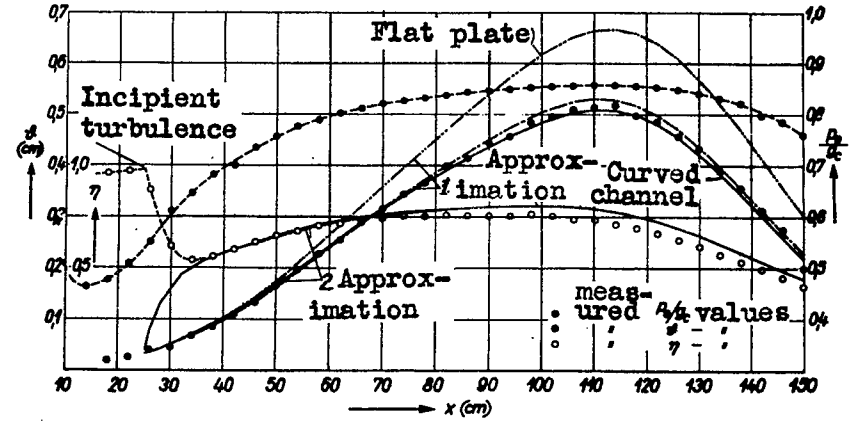

Figure 32.- Set of measurements E

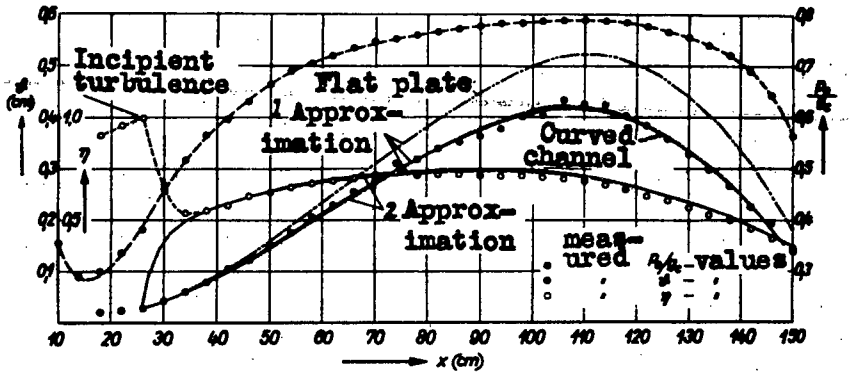

Figure 33.- Set of measurements F.

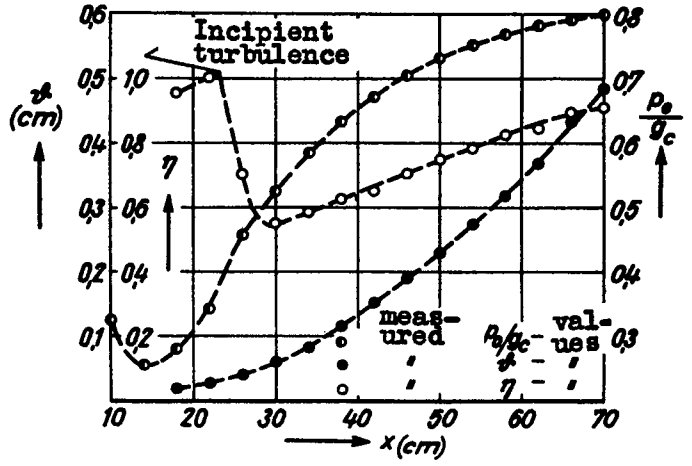

Figure 34.- Set of measurements G.

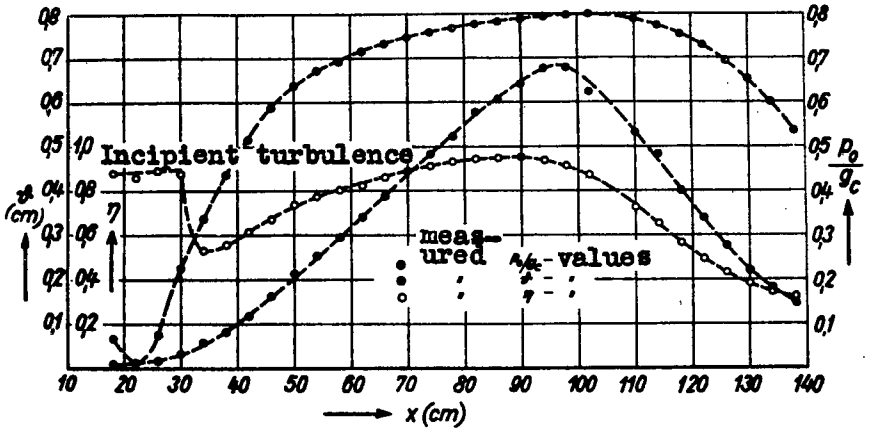

Figure 35.- Set of measurements H.